Int. J. Heat Mass Transfer. Vol. 30, No. 7, pp. 1427–1434, 1987
Printed in Great Britain

0017-9310/87 $3.00 + 0.00

Two-phase downflow in a vertical pipe and the phenomenon of choking: homogeneous diffusion model

Z. BILICKI,† J. KESTIN and J. MIKIELEWICZ†
Division of Engineering, Brown University, Providence, RI 02912, U.S.A.

(*Received* 19 *September* 1986 *and in final form* 1 *December* 1986)

Abstract—The paper analyzes downward two-phase flow of water and its vapor in a vertical pipe exposed to a uniform gravitational field. The flow is assumed to be adiabatic and one-dimensional. The mathematical model used is the equilibrium, homogeneous diffusion model. The study is an application of methods used for dynamical systems and is geometrical–topological in nature. The key to the argument is the determination of the singular and turning points of the governing equations with the help of which it becomes possible to sketch the 'portrait' of trajectories (solution curves) in the phase space composed of pressure P, enthalpy h, and coordinate z, with the mass-flow rate G treated as a parameter. The analysis shows that choking can set-in only at the end of the channel and a critical cross-section inside it is impossible.

INTRODUCTION

THE MOTIVATION for this paper was a desire to understand the phenomena which occur in geothermal wells, with emphasis on choking. In an earlier paper, [1], we examined upward flows in which the shearing stress and gravitational acceleration were codirectional. In this paper we analyze downward flows which characterize reinjection wells, now mandatory in geothermal installations to mitigate subsidence. We continue to employ the homogeneous diffusion model which seems to be adequate for our purpose and confine our analysis to steady, adiabatic, equilibrium flows in vertical channels of constant cross-section. We continue to make use of geometrical methods whose aim it is to describe all possible patterns of solution curves (trajectories) by examining their topological structure in phase space without actually solving the system of differential equations. Such an analysis is very useful as a guide for the organization of numerical solutions by computer.

In this study we present a specific application of a very general method, discussed in detail in ref. [2]. The field of applications of the general method is not restricted to the homogeneous flow model or to adiabatic walls and prevalence of equilibrium between the two phases stipulated in the present study. Thus, this analysis may prove itself to be useful in other applications too, notably in nuclear engineering.

The key to the argument is the study of the mathematical characteristics of points in phase space and their classification into regular points, turning points and singular points. We recall that turning points are associated with choking at the end of a channel. The general analysis shows that only three types of singular points (saddle points, nodal points, spirals) are likely to be encountered, regardless of the complexity of the mathematical model employed. Saddle points and nodal points (but not spirals) signify the appearance of a choked section in the interior of the channel.

In the case of upward flow, ref. [1], no trajectories contained singular points, and turning points corresponded to choking at the upper end of the pipe. The accelerating action of gravitation in the present case suggests that downward flow may be different. In particular, we shall try to discover whether this channel can choke other than at exit.

THE PROBLEM IN THE PHYSICAL SPACE

The nature of the problem in the physical space is illustrated in Fig. 1. We are given a vertical adiabatic pipe of constant area $A = \pi D^2/4$ and length L through which there flows downwards, but in the positive z-direction, and in steady state, a fluid which may evaporate or condense. In our examples this will be water and steam in thermodynamic equilibrium. The terrestrial gravitation g has the same direction as the velocity w and hence the shearing stress τ_w at the wall is opposite to it. We are to determine all flows against a given back-pressure P_a maintained outside $z_e = L$ and to identify the subset of initial conditions which may occur at the entrance $z_1 = 0$, the flow having expanded isentropically through the very short *convergent* section from a stagnation state 0 with $w_0 = 0$. The state of the system is described by the fields

$$P(z),\ h(z),\ \text{and } G = \text{const. as a parameter}$$

where $G = \dot{m}/A$ is the specific flow rate. The former two constitute the dependent functions of the problem. The external pressure P_a must be equal to or lower than the exit pressure P_e at $z_e = L$, and the

† Permanent address: Institute for Fluid Flow Machinery, Polish Academy of Sciences, 80-952 Gdansk, Poland.

NOMENCLATURE

A_{ij}	matrix defined in equation (4)
a	speed of sound
b_i	vector defined in equation (4)
$C_{1,2}$	quantities defined in equations (2a) and (2b)
D	pipe diameter, divergence
$\mathscr{D}$	discriminant, equation (11c)
f	friction factor
G	mass flux density
g	acceleration due to gravity
H	defined in equation (6b)
h	specific enthalpy
J	Jacobian
L	pipe length
$\dot{m}$	mass-flow rate
P	pressure
$\mathscr{S}$	singular point
s	specific entropy
T	temperature
$\mathbf{V}$	directional vector
v	specific volume
w	barycentric velocity
x	dryness fraction
z	coordinate in flow direction.

Greek symbols

α	void fraction
Γ	phase space (Γ_1 subcritical, Γ_2 supercritical)
γ	ratio of specific heats
Δ	determinant, equation (6c)
η	characteristic direction
Π	defined in equation (6a)
ρ	density
$\boldsymbol{\sigma}, \sigma_i$	state vector.

Subscripts

a	external
e	at exit
L	liquid
w	at wall.

Superscripts

$'$	liquid
$''$	vapor
*	at singular point.

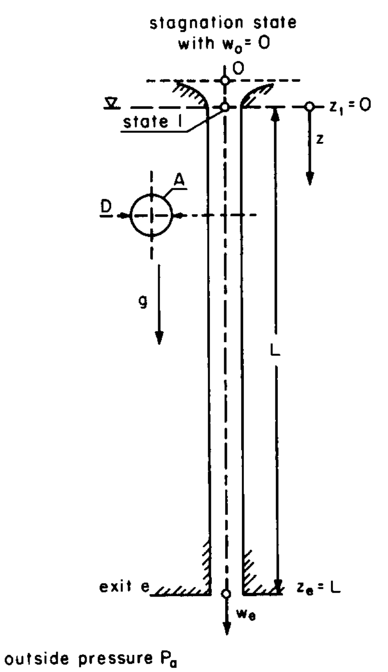

FIG. 1. The physical problem. Note that P_e need not be equal to P_a, but $P_e \geqslant P_a$.

variation of $\dot{m} = GA$ with P_a, not necessarily equal to P_e, is of interest for choking: when it attains its largest value at constant stagnation conditions, the flow is choked.

WORKING EQUATIONS

With the choice of state variables made earlier, we can transcribe the usual conservation equations (see, e.g. ref. [1] or any standard text) to the form:

$$\frac{dG^2}{dz} = 0 \qquad (1a)$$

$$+\left[1 - \frac{G^2 C_1}{\rho^2}\right]\frac{dP}{dz} - \frac{G^2 C_2}{\rho^2}\frac{dh}{dz} = -\frac{2fG^2}{D\rho} + g\rho \qquad (1b)$$

$$-\frac{G^2 C_1}{\rho^3}\frac{dP}{dz} + \left[1 - \frac{G^2 C_1}{\rho^3}\right]\frac{dh}{dz} = g. \qquad (1c)$$

This form is very convenient for analysis with G^2 chosen as a variable parameter. Here

$$C_1 = (\partial\rho/\partial P)_h \quad (\text{always} > 0);$$
$$C_2 = (\partial\rho/\partial h)_P \quad (\text{always} < 0) \qquad (2a,b)$$

except for anomalous regions in the thermodynamic state diagram, ref. [3]. The equation of state is that of the flowing substance, usually available in the form of tables or computer codes. We use the internationally approved Steam Tables [4].

Equation (1b) incorporates the simplest possible closure condition

$$\tau_w = f\rho w^2/2 = f\,G^2/2\rho \qquad (3)$$

with f a constant.

The system of equations (1a)–(1c) is of the standard form

$$A_{ij}\frac{d\sigma_i}{dz} = b_j \quad (4)$$

studied extensively in ref. [2].

THE MATHEMATICAL PROBLEM

Equations (1a)–(1c) constitute a set of coupled, non-linear, first-order, ordinary differential equations conceived as functions of the single independent variable z, and parametrized with respect to G^2. Consequently, the analysis can be carried out in a phase space Γ consisting of only three dimensions: h, P, z. A trajectory (solution) is the vector function $\boldsymbol{\sigma}(z)$, where its components h and P together with the parameter G^2 determine the *state* in a cross-section.

By Cramer's rule, we can write down the following equivalent form of system (1a)–(1c):

$$\frac{dP}{dz} = \frac{\Pi(G^2; P, h)}{\Delta(G^2; P, h)} \quad (5a)$$

$$\frac{dh}{dz} = \frac{\Pi(G^2; P, h)}{\Delta(G^2; P, h)}. \quad (5b)$$

Here

$$\Pi = -\frac{2fG^2}{D\rho}\left(1 - \frac{G^2 C_2}{\rho^3}\right) + \rho g \quad (6a)$$

$$H = -\frac{2fG^4}{D}\cdot\frac{C_1}{\rho^4} + g \quad (6b)$$

with the determinant of the matrix of equations (1a)–(1c)

$$\Delta = 1 - \frac{G^2}{\rho^3}(\rho C_1 + C_2). \quad (6c)$$

THE PHASE SPACE

Equations (5a) and (5b) can be interpreted in the phase space Γ, Fig. 2, as defining a vector field $\mathbf{V}(h, P, z)$ whose elements are everywhere tangent to a trajectory, such as m in the figure. The components of $\mathbf{V}$ are: Π in the P-direction, H in the h-direction and Δ in the z-direction.

The study of the vanishing of the three components, i.e. the loci $\Pi = 0$, $H = 0$, and $\Delta = 0$, is central to our analysis. All three loci are cylinders in Γ, because they do not depend on z explicitly, and the relationships between them can be clearly depicted by drawing their traces in the thermodynamic h, P diagram which forms the base of Γ, Figs. 3 and 4.

Any line parallel to the z-axis in phase space is the intersection of some three cylinders H-const., Π = const., Δ = const., and constitutes, therefore, an isocline, that is the locus of vectors $\mathbf{V}$ of a given magnitude and direction. Thus, if necessary, it is possible to apply the method of isoclines to sketch

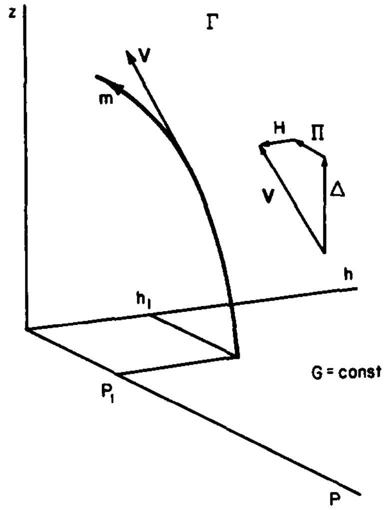

FIG. 2. Typical trajectory m in phase space Γ showing directional vector $\mathbf{V}$ and its components Δ, Π, H.

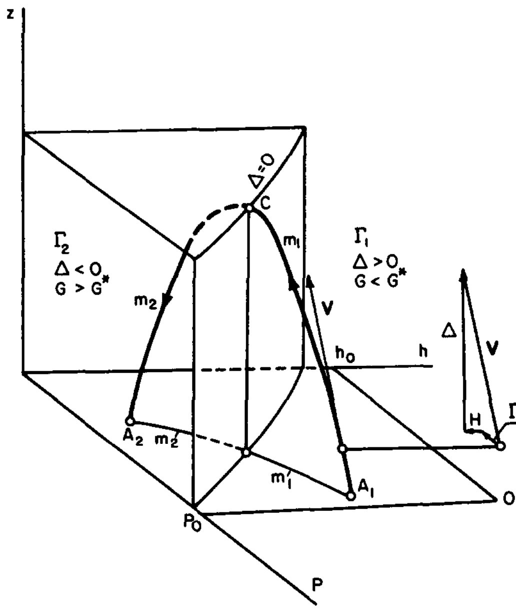

FIG. 3. Subspace Γ (G = const.).

solutions. A more elaborate, but more convenient representation is discussed in the sequel.

The cylinder $\Delta = 0$, Fig. 3, divides Γ into two subspaces. On cylinder $\Delta = 0$ the mass-flow rate acquires the critical value

$$G^* = \rho/(C_1 + C_2/\rho)^{1/2} \quad (7)$$

and the considerations of ref. [1] show that all velocities on this cylinder are equal to the local sound velocity

$$a = (C_1 + C_2/\rho)^{-1/2} \equiv [(\partial P/\partial \rho)_s]^{1/2} \quad (7a)$$

i.e. the velocity of propagation of pressure waves of small amplitude and long wavelength. In subspace Γ_1

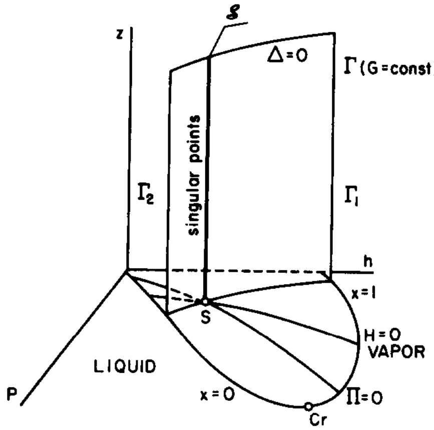

FIG. 4. Singular points in Γ.

with $\Delta > 0$ ($G < G^*$) the limb m_1 of curve m ascends in the z-direction, whereas its limb m_2 descends in $\Gamma_2(G > G^*)$. It follows that $\Delta = 0$ is the locus of all *turning points*. Any curve m which intersects the cylinder $\Delta = 0$ from below must do so with a tangent perpendicular to the z-axis and must attain a maximum in z there, *provided that* Π *and* H do not *vanish at this point simultaneously with* Δ. We note that:

(a) All flows in Γ_1 are subcritical.

(b) All flows in Γ_2 are supercritical.

(c) At all points on $\Delta = 0$ the local flow velocity is that of sound, equation (7a).

(d) Since in the physical space we must have $dz > 0$, curve m can only be traversed along m_1 in the direction of $\mathbf{V}(\Delta > 0)$ or along m_2 in the direction of $-\mathbf{V}$. The possibility of shock formation in Γ_2 is disregarded as being of no importance at present, given that only subcritical flows can set in from a stagnation point with $w_0 = 0$ and convergent entrance, Fig. 1.

In ref. [1] the vector components Π and H were of one sign, always negative in Γ_1. At present both can change sign, equations (6a) and (6b). It can be proved by matrix algebra (see refs. [1, 2]) that the vanishing of H or Π alone on $\Delta = 0$ cannot occur. Thus either

$$H = 0 \text{ } and \text{ } \Pi = 0 \quad \text{on} \quad \Delta = 0 \tag{8a}$$

or

$$H \neq 0 \text{ } and \text{ } \Pi \neq 0 \quad \text{on} \quad \Delta = 0. \tag{8b}$$

In other words, the three cylinders $H = 0$, $\Pi = 0$ and $\Delta = 0$ *must* intersect along a single line $\mathscr{S}$, Fig. 4. Along this line equations (5a) and (5b) fail to determine the components of $\mathbf{V}$. This, then, is the locus of the *singular points* of the system. The angles with which a trajectory crosses $\Delta = 0$ at $\mathscr{S}$ must be determined by other means, and depends on the topological nature of the singular point. No such possibilities existed in upflow.

In the general case, the character of the singular point is obtained by local linearization. In this simple case it is convenient to apply an equivalent but more direct method.

The need to analyze the nature of the singular point arises from the fact that any numerical procedure will fail there, because the system of algebraic equations employed for the numerical solution becomes indeterminate when $H = \Pi = \Delta = 0$ or incompatible when $\Delta = 0$ with $H \neq 0$, $\Pi \neq 0$.

SINGULAR POINTS

Before we proceed to examine the nature of the singular points, we notice that for a given flow rate G there exists a single trace S of $\mathscr{S}$ in h, P, Fig. 4, whose coordinates we denote by h^* and P^*.

Since neither of the components H, Π, Δ depends on z, we seek the projection of the direction $\eta = (\mathrm{d}h/\mathrm{d}P)^*$ along $\mathscr{S}$ into the base plane h, P. We note that along $\mathscr{S}$ $\Delta = 0$, which proves that this is also the direction of $\mathbf{V}$, because vector $\mathbf{V}$ on $\Delta = 0$ must there be normal to z in Γ.

To calculate the slope $\eta = (\mathrm{d}h/\mathrm{d}P)^*$ at any singular point S, we take a Taylor-series expansion† of both H and Π around $S(h^*, P^*)$ and employ de l'Hopital's rule to obtain

$$\eta = \left(\frac{\mathrm{d}h}{\mathrm{d}P}\right)^* = \frac{H_P(G;h^*,P^*)+H_h(G;h^*,P^*)(\mathrm{d}h/\mathrm{d}P)^*}{\Pi_P(G;h^*,P^*)+\Pi_h(G;h^*,P^*)(\mathrm{d}h/\mathrm{d}P)^*}. \tag{9}$$

Here subscripts h and P denote partial differentiation, and the asterisk denotes a value calculated at the singular point S. This is equivalent to the following, quadratic characteristic equation:

$$\Pi_h^*\eta^2 + (\Pi_P^* - H_h^*)\eta - H_P^* = 0. \tag{10}$$

The theory of linear, ordinary differential equations (see, e.g. ref. [5] or any standard text), proves that the nature of the singular point depends on three quantities, the divergence

$$D^* = \Pi_P^* + H_h^* \tag{11a}$$

the Jacobian

$$J^* = \Pi_P^* H_h^* - \Pi_h^* H_P^* \tag{11b}$$

and the discriminant of equation (10), namely

$$\mathscr{D}^* = D^{*2} - 4J^*. \tag{11c}$$

At a *saddle point*

$$\mathscr{D}^* > 0 \quad \text{with} \quad J^* < 0 \tag{12a}$$

at a *nodal point*

† The vanishing of the first-order terms would lead us to a consideration of degenerate singular points which have no practical significance in this context.

Table 1. Locus of singular points S as a function of the parameter G: $f = 0.08$; $D = 0.25$ m

P^* (bar)	α^*	G^* ($kg\ m^{-2}\ s^{-1}$)	$h^* - h_L$ ($kJ\ kg^{-1}$)	h_L ($kJ\ kg^{-1}$)
0.1	0.98	126	15.7	191.8
1.0	0.91	1010	14.8	417.5
2.0	0.84	1857	13.8	504.8
3.0	0.77	2637	12.9	561.6
4.0	0.70	3373	11.9	604.9
5.0	0.64	4076	10.9	640.4
10.0	0.34	7283	5.9	762.9
15.0	0.05	10193	0.8	844.9
15.7	0.01	10586	0.1	854.6
15.8	0.00	10600	0	856.0

h_L—enthalpy on liquid boundary.

$$\mathscr{D}^* > 0 \quad \text{with} \quad J^* > 0 \tag{12b}$$

at a *spiral point*

$$\mathscr{D}^* < 0. \tag{12c}$$

With an equation of state given in tabular or otherwise unwieldy form, it is not possible to establish the appropriate signs other than by systematic, numerical exploration. First, we recall that $\Delta = 0$ implies that $w^* = a^*$ (speed of sound), which in the *liquid region* is of the order of 1500 m s^{-1}. The additional, now sufficient, condition for the existence of a singular point in that region, say $H = 0$, can be derived from equation (6b) with $G = \rho a^*$; we obtain

$$-\frac{2C_1 f a^{*4}}{D} + g = 0. \tag{13}$$

It is not difficult to convince oneself that this condition cannot be met for any reasonable values of f and D. Thus we conclude that reinjection wells which operate without flashing can choke only at the bottom. By contrast, the occurrence of a singular point S situated in the *two-phase region* is not excluded, because then the speed of sound may become as low as $a^* =$ 12 m s^{-1}.

To complete the analysis, we perform numerical calculations for $f = 0.008$, $D = 0.25$ m and trace the movement of point S in the h, P coordinates with the aid of Table 1. It soon transpires that point S is located close to the boundary between the two-phase region and the liquid. This is clear from the small values of $h^* - h_L$, where h_L is the saturation enthalpy. As the mass-flow rate G increases, and the critical pressure P^* increases, S eventually reaches the phase boundary at $P^* = 15.8$ bar, and then crosses into the liquid region where a different equation of state takes over.

All states which correspond to singular points are characterized by a low pressure ($P^* < 15.8$ bar) and very low dryness fraction x^* (order 10^{-2} at 0.1 bar). Nevertheless, the corresponding void fraction

$$\alpha = \frac{xv''}{x(v''-v')+v'} \tag{14}$$

where v is the specific volume (v''-steam, v'-liquid),

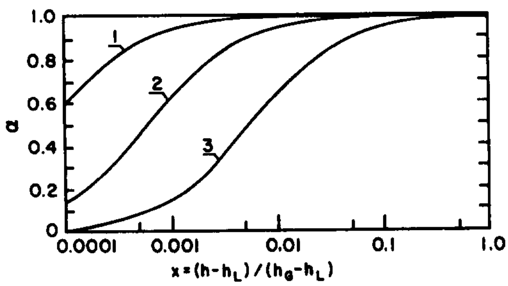

FIG. 5. Relation between void fraction α and dryness fraction x: 1, 0.1 bar; 2, 1.0 bar; 3, 15 bar.

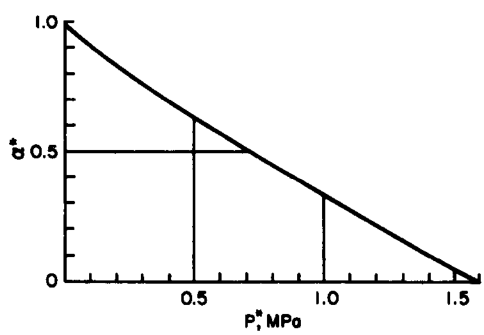

FIG. 6. Variation of dryness fraction with pressure at singular point S when located in the two-phase region.

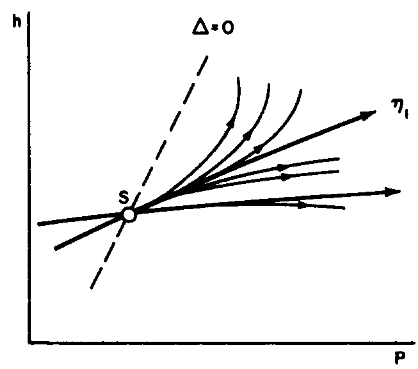

FIG. 7. Topology of nodal point.

ranges over $0 < \alpha < 1$, increasing very rapidly with x in this range, Fig. 5. Consequently, all flow regimes can occur in this range. Naturally, these are potential states *at* the singular point. The states along the trajectories are not so confined. The diagram of Fig. 6 traces the variation of α^* with pressure at S.

A computer-aided probing of conditions (12a)–(12c) indicates that the singular point S in this case is *always a nodal point*. The diagram in Fig. 7 contains a sketch of the trajectories near a typical, nodal point. The two characteristic directions are denoted by η_1 and η_2; they both slope upwards. There is an infinity of trajectories tangent to η_1 and a single trajectory tangent to η_2.

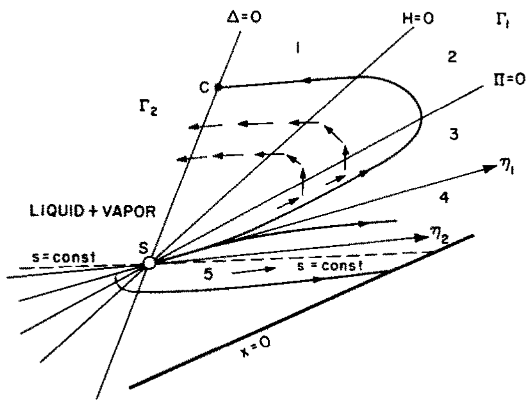

FIG. 8. Vector field **V**.

ENTROPY

The rate of change of entropy is given by the general formula

$$\frac{ds}{dz} = \frac{1}{T}\frac{dh}{dz} - \frac{1}{\rho T}\frac{dP}{dz} \tag{15a}$$

which, in view of the conservation laws, can easily be shown to be equivalent to

$$\frac{ds}{dz} = \frac{4\tau_w}{\rho D T}. \tag{15b}$$

Thus, the requirement of increasing entropy, $ds > 0$, is always satisfied in the flow direction, $dz > 0$.

TRAJECTORIES

We continue to limit attention to the subcritical space $\Gamma_1(\Delta > 0, G < G^*, w < a^*)$.

We can form a clear idea about the topology of trajectories in the two-phase region in two steps. First, we examine the projection $\mathbf{V}'$ of vector field $\mathbf{V}$ into the h, P diagram by an analysis of the loci $\Delta = 0$, $H = 0$ and $\Pi = 0$, Fig. 8. Each of them divides the plane into a negative part and a positive part. Secondly, we introduce the characteristic directions η_1 and η_2 of the nodal point. The relative positions of these lines have been accurately drawn in Fig. 7 which leads us to consider five distinct areas denoted by arabic numerals in the diagram of Fig. 8.

The directions of $\mathbf{V}'$ have been drawn in the diagram in accordance with the equations quoted in the earlier part of this paper. All vectors $\mathbf{V}'$ point in a direction away from S, and this signifies that *a transition from subcritical flow into supercritical flow through the nodal point is impossible*. In fact, state S cannot be reached at all, and its presence merely serves, so to say, to mold the pattern of trajectories. In fact, the vector field $\mathbf{V}'$ forms a vivid basis on which to judge the different types of flow sequences that may be expected to exist.

In any case, it is now quite clear that a downward flow *cannot acquire a choked cross-section other than at the bottom exit*.

More specifically

in area 1	$H < 0$,	$\Pi < 0$;
in area 2	$H > 0$,	$\Pi > 0$;
in areas 3–5	$H < 0$,	$\Pi > 0$.

These signs determine the local directions of vectors $\mathbf{V}'$. A typical trajectory spanning areas 1–3, the latter placed above η_1, is seen sketched in the graph of Fig. 8. On such a trajectory the flow has a maximum enthalpy on $H = 0$ and a maximum pressure on $\Pi = 0$. The flow has a tendency to evaporation and proceeds to an intersection with $\Delta = 0$ at C. If state C (pressure P_C^*) is reached at the end of the pipe, the flow is choked there on condition that $P_a < P_C^*$. If state C falls on the trajectory outside the channel, the flow is not choked at the end, and we can assert that $P_e = P_a$.

In area 4 we encounter an infinity of trajectories which are tangent to η_1. They all move away from $\Delta = 0$ which means that they can never lead to choking. Such flows show a tendency towards condensation, and all such trajectories attain the liquid phase, eventually.

In area 5 we find a single trajectory tangent to η_2 (not shown), as well as trajectories whose origin is in S and which cross $\Delta = 0$ from the supercritical area Γ_2 to the subcritical area Γ_1; their behavior is the same as those in area 4.

It may be worth remembering that all the directions of vectors $\mathbf{V}'$ along $\Delta = 0$ must coincide with $s = \text{const}$. This condition is a consequence of equation (15b) which proves that the sign of ds changes at a turning point from $ds > 0$ along $\mathbf{V}'$ in Γ_1 to $ds < 0$ along $\mathbf{V}'$ in Γ_2.

PERFECT GAS

To conclude the analysis, it is very instructive to draw the phase portrait for the simplest possible equation of state, a perfect gas with constant specific heats, say for $\gamma = 1.3$. Such a variant is not in itself important, because gravitational effects in gases are negligible at all realistic column heights z. Nevertheless, the exercise is instructive for two reasons. First, it is now possible to derive all relations in closed form. Secondly, the full 'portrait' so obtained, being topological in nature, gives a graphical picture of what to expect qualitatively in the presence of more complex equations of state. In this manner, we obtain a fuller picture than the one sketched in Fig. 8.

It is now sufficient simply to quote the equations, because their derivation should be evident. We now record

$$H_P^* = 4a^2\kappa/P^2 > 0 \tag{16a}$$

$$H_h^* = -3a^2\kappa/Ph < 0 \tag{16b}$$

$$\Pi_P^* = \{(3a^2+h)\kappa+\rho hg\}/Ph > 0 \quad (16c)$$

$$\Pi_h^* = -\{(2a^2+h)\kappa+\rho hg\}/h^2 < 0 \quad (16d)$$

where

$$\kappa = \rho g/\gamma, \quad a^2 = (\gamma-1)h \quad (16e,f)$$

$$\rho = \gamma P/(\gamma-1)h. \quad (16g)$$

Hence

$$D^* = \frac{\rho^2}{D^2P^2}[2+(\gamma-1)(3-2\gamma)-Dg]^2 > 0 \quad (17)$$

and

$$J^* = \Pi_P^* H_h^* - \Pi_h^* H_P^* > 0. \quad (18)$$

Referring to equation (12b) we conclude that we encounter here also a nodal point. The characteristic directions are

$$\eta_1 = (9\gamma-8)P/8(\gamma-1)h \quad (19a)$$

$$\eta_2 = [(6\gamma-5)+3(\gamma-1)]P/8(\gamma-1)h. \quad (19b)$$

The preceding equations have been programmed on a computer linked with an automatic plotter. The resulting pattern with $G^* = 2166\ \mathrm{kg\,m^{-2}\,s^{-1}}$, $P^* = 10$ bar, $h^* = 1.2\times10^3\ \mathrm{kJ\,kg^{-1}}$ is shown in Fig. 9.

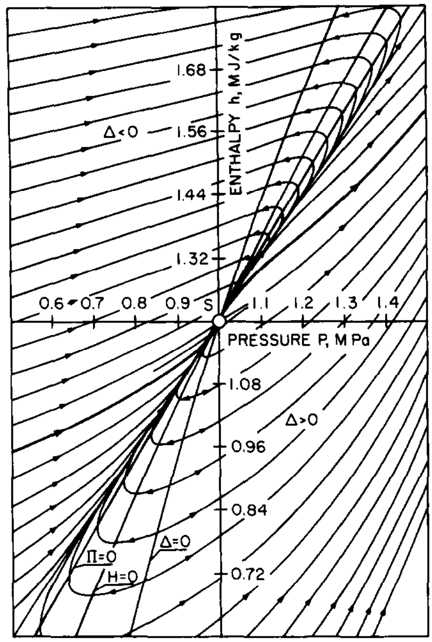

FIG. 9. Portrait in h, P diagram for perfect gas.

CONJECTURE

We recall once more that a mathematical model of two-phase flow consists of three components: a set of conservation laws, a set of closure conditions and an equation of state. The two examples analyzed in this paper, Figs. 8 and 9, resulted in topologically identical 'portraits' of trajectories in phase space. The two cases were based on identical forms of the conservation laws and closure conditions; they differed in the equation of state: the complex equation for steam and water in Fig. 8 and the very simple equation of a perfect gas in Fig. 9. If it could be shown convincingly that the two patterns turned out to be identical other than by coincidence, that is that the forms of the conservation laws and closure conditions impose a topological 'portrait' which is insensitive to the equation of state, in spite of the fact that quantitatively the trajectories are vastly different, we would be able greatly to simplify future analyses.

Acknowledgments—The work presented in this paper is a continuation of an investigation started under the sponsorship of the Division of Geothermal Energy of the U.S. Department of Energy. The present effort was supported by grant No. DE-AC02-84ER-13167 awarded to Brown University by the Office of Energy Engineering Research of the U.S. Department of Energy. Special thanks are due to Dr O. P. Manley, the Project Manager, for his interest and encouragement.

REFERENCES

1. Z. Bilicki and J. Kestin, Two-phase flow in a vertical pipe and the phenomenon of choking: homogeneous diffusion model—I. Homogeneous flow models, *Int. J. Multiphase Flow* **9**, 269–288 (1983).
2. Z. Bilicki, C. Dafermos, J. Kestin, G. Majda and D.-L. Zeng, Trajectories and singular points in steady state models of two-phase flow, *Int. J. Multiphase Flow* (1987), in press.
3. S. L. Rivkin, A. A. Aleksandrov and E. A. Kremenevskaya, *Thermodynamic Derivatives for Water and Steam*. Wiley, New York (1978).
4. L. Haar, J. S. Gallagher and G. S. Kell, *NBS/NRC Steam Tables*. Hemisphere, Washington, DC (1984).
5. J. Kestin and S. K. Zaremba, Geometrical methods in the analysis of ordinary differential equations, *Appl. Scient. Res. Math.* **B3**, 149–189 (1952).

ECOULEMENT DIPHASIQUE DESCENDANT DANS UN TUBE VERTICAL ET PHENOMENE DE CHOC: MODELE DE DIFFUSION HOMOGENE

Résumé—On analyse l'écoulement diphasique d'eau liquide et de vapeur qui descend dans un tube vertical avec un champ gravitationnel uniforme. L'écoulement est supposé être adiabatique et monodimensionnel. Le modèle mathématique utilisé est un modèle d'équilibre et de diffusion homogène. L'étude est une application de méthodes utilisées pour les systèmes dynamiques et il est de nature géométrique et topologique. La clef de l'argument est la détermination des points singuliers et de retournement des équations qui rend possible la description des trajectoires dans l'espace de phase composé de la pression P, de l'enthalpie h et de la coordonnée z, avec le débit masse spécifique G traité comme un paramètre. L'analyse montre qu'un choc peut s'installer seulement à l'extrémité du canal et qu'une section critique à l'intérieur est impossible.

ZWEIPHASENABWÄRTSSTRÖMUNG IN EINEM SENKRECHTEN ROHR UND DAS PHÄNOMEN DER AUFSTAUUNG: DAS HOMOGENE DIFFUSIONSMODELL

Zusammenfassung—Es wird die abwärtsgerichtete Zweiphasenströmung aus Wasser und Wasserdampf in einem senkrechten Rohr in einem gleichförmigen Gravitationsfeld untersucht. Die Strömung wird als adiabat und eindimensional betrachtet. Als mathematisches Modell wird das homogene Diffusionsmodell verwendet. Es werden Methoden, die für dynamische Systeme angewandt werden, eingesetzt. Das Modell ist geometrisch-topologischer Natur. Bestimmt werden Singularitäten und Wendepunkte der Erhaltungsgleichungen, mit deren Hilfe es möglich wird, das "Porträt" der Trajektorien (Lösungskurven) im Phasenraum zu zeichnen, die sich aus dem Druck P, der Enthalpie h und der Koordinate z zusammensetzen, mit der Massenstromdichte G als Parmeter. Die Untersuchung zeigt, daß Aufstauung nur am Ende des Rohres auftreten kann und daß ein kritischer Querschnitt innerhalb unmöglich ist.

ДВУХФАЗНЫЙ НИСХОДЯЩИЙ ПОТОК В ВЕРТИКАЛЬНОЙ ТРУБЕ И ЯВЛЕНИЕ ДРОССЕЛИРОВАНИЯ: ГОМОГЕННАЯ ДИФФУЗИОННАЯ МОДЕЛЬ

Аннотация—Исследуется двухфазный нисходящий поток воды и водяного пара в вертикальной трубе, помещенной в однородное гравитационное поле. Течение считается адиабатическим и одномерным. В качестве математической модели выбрана равновесная гомогенная диффузионная модель. Применяются геометро-топологические методы, используемые для динамических систем. Определены сингулярные точки возврата определяющих уравнений, что позволяет получить «портрет» траекторий (кривых решения) в фазовом пространстве давления P, энтальпии h и координаты z (массовый расход G рассматривается как параметр). Анализ показывает, что дросселирование может возникнуть только в конце канала, а существование критического сечения внутри него невозможно.